JOURNAL OF VIROLOGY, May 2010, p. 4714–4724 Vol. 84, No. 9
0022-538X/10/$12.00 doi:10.1128/JVI.02633-09

In Vivo Tropism of Attenuated and Pathogenic Measles Virus Expressing Green Fluorescent Protein in Macaques▽

Rory D. de Vries,[1] Ken Lemon,[2] Martin Ludlow,[1] Stephen McQuaid,[3] Selma Yüksel,[1] Geert van Amerongen,[1] Linda J. Rennick,[2] Bert K. Rima,[2] Albert D. M. E. Osterhaus,[1] Rik L. de Swart,[1]* and W. Paul Duprex[2]

Department of Virology, Erasmus MC, Rotterdam, Netherlands[1]; Centre for Infection and Immunity, School of Medicine, Dentistry and Biomedical Sciences, Queen's University of Belfast, Belfast, United Kingdom[2]; and Tissue Pathology, Belfast Health and Social Care Trust, Queen's University of Belfast, Belfast, United Kingdom[3]

Received 16 December 2009/Accepted 12 February 2010

The global increase in measles vaccination has resulted in a significant reduction of measles mortality. The standard route of administration for the live-attenuated measles virus (MV) vaccine is subcutaneous injection, although alternative needle-free routes, including aerosol delivery, are under investigation. *In vitro*, attenuated MV has a much wider tropism than clinical isolates, as it can use both CD46 and CD150 as cellular receptors. To compare the *in vivo* tropism of attenuated and pathogenic MV, we infected cynomolgus macaques with pathogenic or attenuated recombinant MV expressing enhanced green fluorescent protein (GFP) (strains IC323 and Edmonston, respectively) via the intratracheal or aerosol route. Surprisingly, viral loads and cellular tropism in the lungs were similar for the two viruses regardless of the route of administration, and CD11c-positive cells were identified as the major target population. However, only the pathogenic MV caused significant viremia, which resulted in massive virus replication in B and T lymphocytes in lymphoid tissues and viral dissemination to the skin and the submucosa of respiratory epithelia. Attenuated MV was rarely detected in lymphoid tissues, and when it was, only in isolated infected cells. Following aerosol inhalation, attenuated MV was detected at early time points in the upper respiratory tract, suggesting local virus replication. This contrasts with pathogenic MV, which invaded the upper respiratory tract only after the onset of viremia. This study shows that despite *in vitro* differences, attenuated and pathogenic MV show highly similar *in vivo* tropism in the lungs. However, systemic spread of attenuated MV is restricted.

Measles virus (MV) is one of the most contagious human viruses and is transmitted via aerosols or by direct contact with contaminated respiratory secretions. Clinical symptoms appear approximately 2 weeks after infection and include fever, rash, cough, coryza, and conjunctivitis (20). Measles is associated with immunosuppression, resulting in increased susceptibility to opportunistic infections. While significant progress has been made in global control programs, 164,000 deaths were attributed to measles in 2008 (46).

MV was first isolated in cell culture in 1954 (16). This Edmonston wild-type MV strain was passaged multiple times in primary human kidney and amnion cells and adapted to eggs and chicken embryo fibroblasts to produce the live-attenuated Edmonston-B vaccine virus (15), which was later replaced by the more attenuated MV strains (Edmonston-Zagreb, Moraten, and Schwarz) (34). These vaccines have been shown to be safe and effective, and high coverage in two-dose regimens has successfully interrupted endemic MV transmission in large geographic areas (6).

For many years, laboratory-adapted MV-Edmonston strains were used as the prototype virus and were shown to display a wide cellular tropism *in vitro*. The virus efficiently infected epithelial cells, which were considered the target cells for primary MV infection *in vivo* (22). In 1993, the cell surface glycoprotein CD46, expressed by virtually all nucleated human cells, was identified as a cellular receptor for MV (11, 26). However, it became evident that only vaccine and laboratory-adapted MV strains were able to utilize this molecule as a cellular receptor (4). CD150, a membrane glycoprotein expressed on subsets of lymphoid and myeloid cells, was identified as the receptor for wild-type MV strains in 2000 (40, 47).

Experimental infections of nonhuman primates with the Edmonston wild-type MV have given variable results: initial studies reported clinical signs, including rash (30), but later studies suggested that these viruses were in fact attenuated (3, 45). It is now known that most MV strains isolated in CD150-negative cells are attenuated *in vivo*, whereas non-cell-culture-passaged MV or wild-type strains isolated and passaged in CD150-positive cells retain pathogenicity (for a review, see reference 7). We recently infected macaques with a recombinant MV based on the IC323 strain expressing a fluorescent protein (21, 39), a virus that exclusively uses CD150 as a cellular receptor. This virus retained its pathogenicity in nonhuman primates, and CD150-expressing lymphocytes and dendritic cells (DC) were the predominant target cells for MV replication (9).

Although attenuated MV strains have been used successfully in large-scale vaccination campaigns, surprisingly little is known about the molecular mechanisms underlying this attenuation. In addition to having a wider tropism *in vitro*, attenuated MV strains have deficiencies in their capacity to antagonize innate immune responses (27). Experimental infections in nonhuman primates demonstrated that attenuated MV may

* Corresponding author. Mailing address: Department of Virology, Erasmus MC, P.O. Box 2040, 3000 CA, Rotterdam, Netherlands. Phone: 31-10-7044280. Fax: 31-10-7044760. E-mail: r.deswart@erasmusmc.nl.
▽ Published ahead of print on 24 February 2010.

cause low-level viremia, although virus loads were 10- to 100-fold lower than those observed in animals infected with pathogenic MV (3, 45) and in some cases were undetectable (8). However, nothing is known about the cell types and tissues targeted by attenuated MV strains *in vivo*. This subject has gained importance in recent years due to activities aimed at developing alternative needle-free routes of measles vaccination (42).

In the present study, we aimed to compare the *in vivo* tropism of attenuated and pathogenic MV using two recombinant MV strains expressing enhanced green fluorescent protein (EGFP): rMV^{rEdt}EGFP, a clone of the Edmonston-tag (Edtag) virus (32) that contains a repaired phosphoprotein (P) gene (L. J. Rennick et al., unpublished data), and rMV^{IC323}EGFP (21), which was previously used in pathogenesis studies of macaques (9). rMV^{rEdt}EGFP can use both CD46 and CD150 as cellular receptors *in vitro*, whereas rMV^{IC323}EGFP exclusively uses CD150 as a cellular receptor. In the majority of previous experimental MV infections of macaques, we used intratracheal (i.t.) inoculation as the route of virus administration. The main advantage of this route is that it ensures delivery of the complete virus dose to the lungs. However, there is a clear disadvantage in that it does not mimic the natural route of MV transmission. In the present study, we compared i.t. inoculation and aerosol inhalation in order to overcome this limitation and better understand how the virus is able to establish a natural infection.

MATERIALS AND METHODS

Cells and viruses. For the scope of this study, an attenuated and a pathogenic MV expressing EGFP were used. The attenuated MV was based on the first molecularly cloned MV strain, the Edtag virus (32). The Edtag strain of MV has historically been used for *in vivo* MV studies (29, 41, 43). The V protein of the Edtag strain has been shown to be defective in counteracting interferon (IFN) signaling pathways due to tyrosine-to-histidine and cysteine-to-arginine substitutions at amino acid positions 110 and 272, respectively (10, 17, 28). The presence of a functional V protein is crucial for establishing a productive infection *in vivo* (10). For this reason, the P gene of the recombinant Edtag virus was replaced with that of an early-passage Edmonston vaccine strain (19) (GenBank accession number GU327676). This gene encodes a V protein that is identical to that of the Moraten vaccine strain of MV, which has been shown to be competent for antagonizing the IFN signaling pathway (10). Upon rescue, this virus was shown to have a normal V protein and stable EGFP expression and was designated rMV^{rEdt}EGFP (Rennick et al., unpublished). As a pathogenic MV, we used rMV^{IC323}EGFP, the *in vivo* virulence of which has been previously validated in the macaque model (9). Virus stocks were grown in an Epstein-Barr virus-transformed human B-lymphoblastic cell line (B-LCL) and tested negative for contamination with *Mycoplasma* species. Virus titers were determined by endpoint titration in Vero-CD150 cells and were expressed as 50% cell culture infectious doses ($CCID_{50}$).

***In vitro* infection of primary human cells.** Peripheral blood mononuclear cells (PBMC) were isolated from human blood by density gradient centrifugation. T lymphocytes were expanded by stimulation of PBMC with phytohemagglutinin (PHA-L) in the presence of interleukin 2 (IL-2) (50 IU/ml); B lymphocytes were isolated with CD19 magnetic beads and expanded by coculture with gamma-irradiated murine L cells expressing human CD40L (18) in the presence of recombinant human IL-4 (40 IU/ml); monocytes were isolated by CD14 magnetic-bead separation and differentiated into immature DC and macrophages. Immature monocyte-derived DC were obtained by culturing monocytes for 5 days in the presence of IL-4 (300 IU/ml) and granulocyte-macrophage colony-stimulating factor (GM-CSF) (300 IU/ml), whereas to obtain macrophages, the monocytes were cultured in the presence GM-CSF only. Immature DC were differentiated by stimulation with a maturation mixture containing tumor necrosis factor alpha (TNF-α), IL-6, IL-1β1, and prostaglandin E_2 (PGE_2), as described previously (1). Different cell types were infected with either rMV^{rEdt}EGFP (attenuated) or rMV^{IC323}EGFP (pathogenic) MV at a multiplicity of infection (MOI) of 0.01 and cultured for 3 days. The percentages of MV-infected cells were measured by flow cytometry at 24, 48, and 72 h postinfection (p.i.) by measuring the percentage of EGFP$^+$ cells on a FACSCanto II. Measurements were performed in triplicate on cells obtained from two different blood donors. Prior to infection, all cell types were analyzed for expression of the MV receptors CD46 and CD150 by flow cytometry with appropriate isotype controls performed in parallel.

Ex vivo infection of macaque spleen cells. Spleens were collected from three rhesus macaques, which had been sacrificed in the framework of another study. The spleens were minced, and single-cell suspensions were prepared using cell strainers with a 100-μm pore size (BD Biosciences); mononuclear cells were obtained by density gradient centrifugation. The cells were infected with either attenuated or pathogenic MV at an MOI of 0.1 and cultured for 4 days. Infection percentages were measured in duplicate by flow cytometry at 24, 48, and 96 h p.i.

Animal study design. Juvenile MV-seronegative cynomolgus macaques were housed in negatively pressurized, HEPA-filtered biosafety level 3 (BSL-3) isolator cages. The animals were infected with either rMV^{IC323}EGFP (groups A and B; $n = 8$) or rMV^{rEdt}EGFP (groups C and D; $n = 8$). Within these two groups, four animals were infected with 10^4 $CCID_{50}$ by i.t. inoculation (groups A and C), and four animals were infected by aerosol inhalation (groups B and D). Aerosol was generated using the Aeroneb Lab nebulizer with an OnQ aerosol generator (kind gift of J. Fink, Nektar Therapeutics). Previous studies had shown that this combination efficiently delivers an aerosol to the airways of nonhuman primates, depositing over 10% of the generated aerosol into the lungs (12). In order to optimize the infectious dose of virus, the virus was titrated on Vero-CD150 cells before and after bench nebulization. This showed an approximate 2-fold decrease in the amount of infectious virus (data not shown). Therefore, we hypothesized that exposing the macaques to a dose of 10^6 $CCID_{50}$ of nebulized virus corresponded to an approximate i.t. dose of 10^4 $CCID_{50}$. This corrected for the limited deposition into the lungs, virus loss by nebulization, loss of the aerosol into the environment, aerosol deposition on the skin and eyes, and aerosol that was swallowed during nebulization. All animals were euthanized on day 7, which we estimated to be the peak of attenuated-MV replication and shortly before the peak of pathogenic-MV replication. This study was approved by the animal ethics committee and performed according to Dutch guidelines for animal experimentation.

Samples. Small-volume EDTA blood samples were collected in Vacuette tubes containing K3EDTA as an anticoagulant 0, 2, 4, 5, 6, and 7 days p.i. Plasma was separated from the blood by centrifugation, heat inactivated (30 min; 56°C), and stored at −20°C. White blood cells (WBC) were obtained by direct treatment of EDTA blood with red blood cell lysis buffer (Roche Diagnostics, Penzberg, Germany). WBC were resuspended in complete RPMI 1640 medium (Gibco Invitrogen, Carlsbad, CA) supplemented with L-glutamine (2 mM), 10% (vol/vol) heat-inactivated fetal bovine serum (FBS), penicillin (100 U/ml), and streptomycin (100 μg/ml); counted using a hemocytometer; and used directly for virus isolation and flow cytometry. PBMC were isolated from EDTA blood 0, 6, and 7 days p.i. by density gradient centrifugation; resuspended in culture medium as described above; and used for virus isolation and flow cytometry. A bronchoalveolar lavage (BAL) was performed 6 days p.i. by i.t. infusion of 10 ml phosphate-buffered saline (PBS) through a flexible catheter. On day 7 p.i., a BAL was performed postmortem by direct infusion of 10 ml PBS into the right lung lobe. BAL cells were resuspended in culture medium with supplements as described above, counted, and used directly for virus isolation. The remaining BAL cells were directly analyzed for EGFP expression by UV microscopy. Throat and nose swabs were collected 0, 2, 4, 5, 6, and 7 days p.i. for both virus isolation and virus detection by real-time reverse transcription (RT)-PCR (13).

Virus detection. Isolation of MV was performed on human B-LCL using an infectious-center test as previously described (14). Virus isolations were monitored by UV microscopy for EGFP fluorescence after cocultivation with B-LCL for 3 to 6 days. The results are expressed as the number of virus-infected cells per 10^6 total cells. Real-time RT-PCR on throat and nose swabs was performed as described previously (13).

Macroscopic detection of EGFP fluorescence. Macroscopic detection of EGFP was performed as described previously (9). Briefly, fluorescence was detected with a custom-made lamp containing 6 LEDs (peak emission, 490 to 495 nm); the emitted fluorescence was detected through an amber cover of a UV transilluminator used for screening DNA gels. Photographs were made using a Nikon D80 SLR camera.

Necropsies. Animals were euthanized by sedation with ketamine (20 mg/kg body weight), followed by exsanguination. Samples were collected in 4% (wt/vol) paraformaldehyde (PFA) in PBS (to preserve EGFP autofluorescence) or in buffered formalin. Representative blocks from the upper, intermediate, and lower lung were sampled to provide maximum surface area. A selection of

samples was also collected in PBS for direct processing of tissues or was snap-frozen in liquid nitrogen and stored at −80°C.

Flow cytometry. Freshly isolated WBC and PBMC were stained with monoclonal antibodies raised against human antigens and cross-reactive with macaque cell surface markers. T lymphocytes were detected by staining them with CD3 (BD Pharmingen; clone SP34-2) and subdivided into CD4 (NIH; clone L200) and CD8 (Dako; clone DK25). B lymphocytes were identified using HLA-DR (BD Biosciences; clone L243) and CD20 (BD Biosciences; clone L27) monoclonal antibodies. EGFP was always detected in the fluorescein isothiocyanate (FITC) channel. Fluorescence was measured on a FACSCanto II, obtaining approximately 10^6 events to allow detection of low-frequency $EGFP^+$ populations. Lymphoid tissues, collected in PBS, were minced, and single-cell suspensions were prepared using cell strainers with a 100-μm pore size (BD Biosciences); the cells were directly used for flow cytometry, after being stained with CD3 and CD20.

Immunohistochemical and immunofluorescence analyses of formalin-fixed tissues. All formalin-fixed sections were deparaffinized, and antigen retrieval was performed in a pressure cooker at full power for 3 min in 0.01 M Tris-EDTA buffer (pH 9.0). MV-infected cells were detected using a polyclonal rabbit antibody to EGFP (Invitrogen). Sections were incubated in primary antibody overnight at 4°C, and specific antibody-antigen binding sites were detected using an Envision-Peroxidase system with DAB (Dako) as a substrate. Dual-labeling indirect immunofluorescence was performed using polyclonal rabbit anti-EGFP and monoclonal mouse antibodies to the myeloid (macrophage/DC) marker CD11c (Novocastra; clone 5D11), the T-lymphocyte marker CD3 (Dako; clone F7.2.38), the B-lymphocyte marker CD20 (Dako; clone L26), and an epithelial cytokeratin cell marker (Dako; clone AE1/AE3). Antigen binding sites were detected with a mixture of anti-mouse Alexa 568 and anti-rabbit Alexa 488 (Invitrogen). Sections were counterstained with DAPI (4′,6′-diamidino-2-phenylindole) hard-set mounting medium (Vector). All fluorescently stained slides were examined at ×200, ×400, and ×1,000 magnifications on a fluorescence imaging microscope (Leica Microsystems).

RESULTS

***In vitro* infections of different cell types.** To compare the *in vitro* potential of the viruses to use CD150 as an entry receptor, Vero or Vero-CD150 cells were infected with $rMV^{rEdt}EGFP$ (attenuated) or $rMV^{IC323}EGFP$ (pathogenic). In Vero cells, pathogenic MV was able to infect single cells, but only at a high MOI and never associated with cytopathic effects (Fig. 1A). Attenuated MV replicated well in Vero cells, resulting in large syncytia irrespective of the MOI. Both viruses efficiently infected Vero-CD150 cells both at high and at low MOIs, resulting in clear cytopathic effects (Fig. 1A).

To compare the *in vitro* susceptibilities of primary human cells of lymphoid and myeloid origin, activated T and B lymphocytes, macrophages, immature DC, and mature DC were infected with either attenuated or pathogenic MV. At the time of infection, all cell types expressed CD46 at a high level, whereas CD150 expression was high on B lymphocytes, lower on T lymphocytes and mature DC, and virtually absent on immature DC and macrophages (Fig. 1B). Infection with attenuated MV resulted in higher percentages of infected cells than infection with pathogenic MV (Fig. 1C). Monocyte-derived macrophages and immature DC showed low infection percentages with pathogenic MV, corresponding to the absence of CD150, but despite the abundant expression of CD46, an analogous restriction in virus replication was also observed with attenuated MV (Fig. 1C).

In order to compare the infectivity of MV for macaque splenocytes, complete spleen cell populations were infected *ex vivo* with either attenuated or pathogenic MV. Using an MOI of 0.1, infection with attenuated MV resulted in 1 to 2% $EGFP^+$ cells 24 h p.i., which remained stable up to 4 days p.i. In contrast, pathogenic MV was barely detectable for the first 2 days p.i., but at day 4, the percentage of $EGFP^+$ cells increased up to 5 to 6% (Fig. 1D).

MV replication after aerosol and i.t. delivery. Macaques were infected in four groups of four animals each with either pathogenic or attenuated MV, via either the i.t. or aerosol route. No clinical signs were observed during the course of the experiment. Virus isolations were performed from PBMC and BAL cells to compare viremia and local replication in the lower respiratory tract. Real-time RT-PCR on throat and nose swabs was performed to detect viral presence in the upper respiratory tract. Pathogenic MV was isolated from PBMC of all eight animals; the virus loads in these samples were comparable for both administration routes (Fig. 2A, right). Clearly, the level of infection was still increasing to 7 days p.i., indicating that the animals were euthanized slightly before the peak of virus replication. Kinetics were similar to those described previously for pathogenic MV infections in macaques (9, 14, 35, 44, 45). In contrast, attenuated MV was isolated only from PBMC of a single animal at a very low level in the aerosol-infected group (Fig. 2A, right). The amounts of virus isolated from BAL cells were comparable after either i.t. or aerosol infection with pathogenic MV, and virus could be isolated from all animals. The BAL from all macaques infected with attenuated MV contained infectious MV at either 6 or 7 days p.i. The numbers of MV-infected cells were comparable after either i.t. or aerosol infection and were approximately 10-fold lower than those observed with pathogenic MV (Fig. 2A, left). UV microscopy was used to confirm the presence of $EGFP^+$ cells in BAL in all cases (data not shown).

Flow cytometry of WBC and PBMC showed that $CD3^+$ $CD4^+$, $CD3^+$ $CD8^+$, and $CD20^+$ cells were infected with pathogenic MV to similar extents after i.t. or aerosol infection, with $CD3^+$ $CD4^+$ cells identified as the primary target cells. Attenuated MV could not be detected in PBMC by flow cytometry (Fig. 2B).

MV was detected by RT-PCR in the upper respiratory tract of all animals infected with $rMV^{IC323}EGFP$, but only after the onset of viremia (day 4 for throat swabs, and day 6 for nose swabs). Viral loads were again comparable for both routes of administration. In attenuated-MV-infected animals, there was a striking difference between the i.t. and aerosol infections. I.t. infection with attenuated MV did not lead to local replication in the nose and throat, whereas infection via the aerosol route led to immediate replication in the upper respiratory tract. Virus could already be detected 2 days p.i. (Fig. 2C). Virus isolations performed with cells from the throat and nose swabs showed similar results (data not shown), indicating that the virus detected by real-time RT-PCR was indeed live infectious virus. However, although pathogenic MV could never be detected in any nose or throat sample at these early time points, it should be noted that the absolute levels that were detected were relatively low compared to those detected at later time points in animals infected with pathogenic MV.

Infection of lymphoid tissues by pathogenic and attenuated MV. Macroscopic fluorescence was detected in all animals following either i.t. or aerosol infection with pathogenic MV. The affected tissues were similar in both groups and included the skin, gingiva, buccal mucosa, tongue, trachea, primary bronchus, lungs, and all lymphoid tissues (lymph nodes, spleen, thymus, tonsils, adenoids, and gut-associated lymphoid tissue)

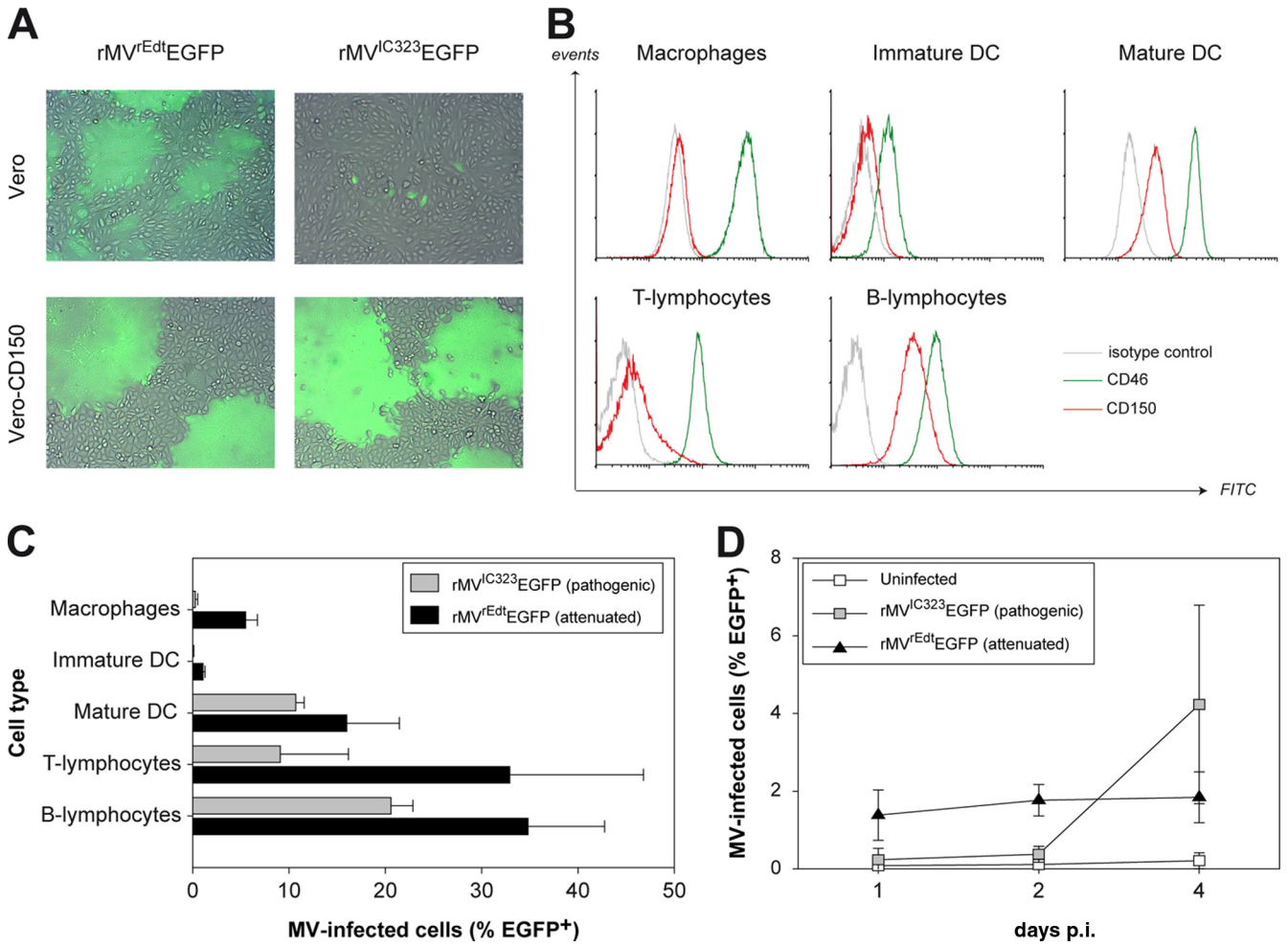

FIG. 1. (A) Infection of Vero and Vero-CD150 cells by attenuated and pathogenic MV. Attenuated MV was capable of infecting and causing cell-cell fusion in Vero and Vero-CD150 cells. Pathogenic MV infected and fused Vero-CD150 cells efficiently, but in Vero cells, only sparse single infected cells were detected. Overlays of normal light and fluorescence micrographs were created using Adobe Photoshop CS3 software. (B) CD46 and CD150 expression on primary human cells. Prior to infection of primary human cells, the levels of CD46 and CD150 surface expression were determined by flow cytometry. (C) Infection of primary human cells. Different cells of lymphoid or myeloid origin were infected *in vitro* with attenuated or pathogenic MV. Infection was measured by flow cytometry at 3 days p.i. The results are shown as means and standard deviations (SD) of triplicate measurements of two different donors. (D) Infection of macaque splenocytes. Macaque splenocytes were infected with attenuated or pathogenic MV, and infection was measured by flow cytometry at 1 to 4 days p.i. The results are shown as means ± SD of duplicate measurements of three different animals.

(data not shown). These tissues correlate with affected tissues described previously (9). Flow cytometry of single-cell suspensions from lymph nodes indicated that $CD20^+$ B lymphocytes were the primary target cells for pathogenic MV in these tissues and again showed no difference between infection via the i.t. or aerosol route (Fig. 3A and B).

In attenuated-MV-infected macaques, macroscopic fluorescence was detected only in the upper and lower respiratory tract; all lymphoid tissues were negative. The absence of attenuated MV in these organs was confirmed by flow cytometry (Fig. 3A and B). Immunohistochemistry revealed virus in lymph nodes from two attenuated-MV-infected macaques, but the numbers of infected cells were very limited in comparison to pathogenic-MV-infected lymph nodes (Table 1 and Fig. 3C and D).

Local MV replication in the lungs. Macroscopically, EGFP was detected in all pathogenic-MV-infected lungs and in the lungs of 2 out of 4 attenuated-MV-infected animals from both the i.t. and aerosol-infected groups. Upon comparison to pathogenic MV, which formed large foci around the edges of the lung lobes, attenuated MV was observed to form smaller $EGFP^+$ foci of infection throughout the lungs (Fig. 4). Microscopically, the presence of MV in the lungs was detected in all animals (Table 1). Little difference was observed between infected cells observed in the parenchyma of the lungs of pathogenic- and attenuated-MV-infected animals (Fig. 5 and 6). However, in the lungs of animals infected with pathogenic MV, many EGFP-positive cells were found in infiltrating immune cells, whereas these cells were much less infected by attenuated MV (Fig. 3E and F, respectively).

Attenuated MV infects cells of lymphoid, myeloid, and epithelial origin in the lungs. Indirect-immunofluorescence dual labeling was performed on lung tissues from both i.t. and

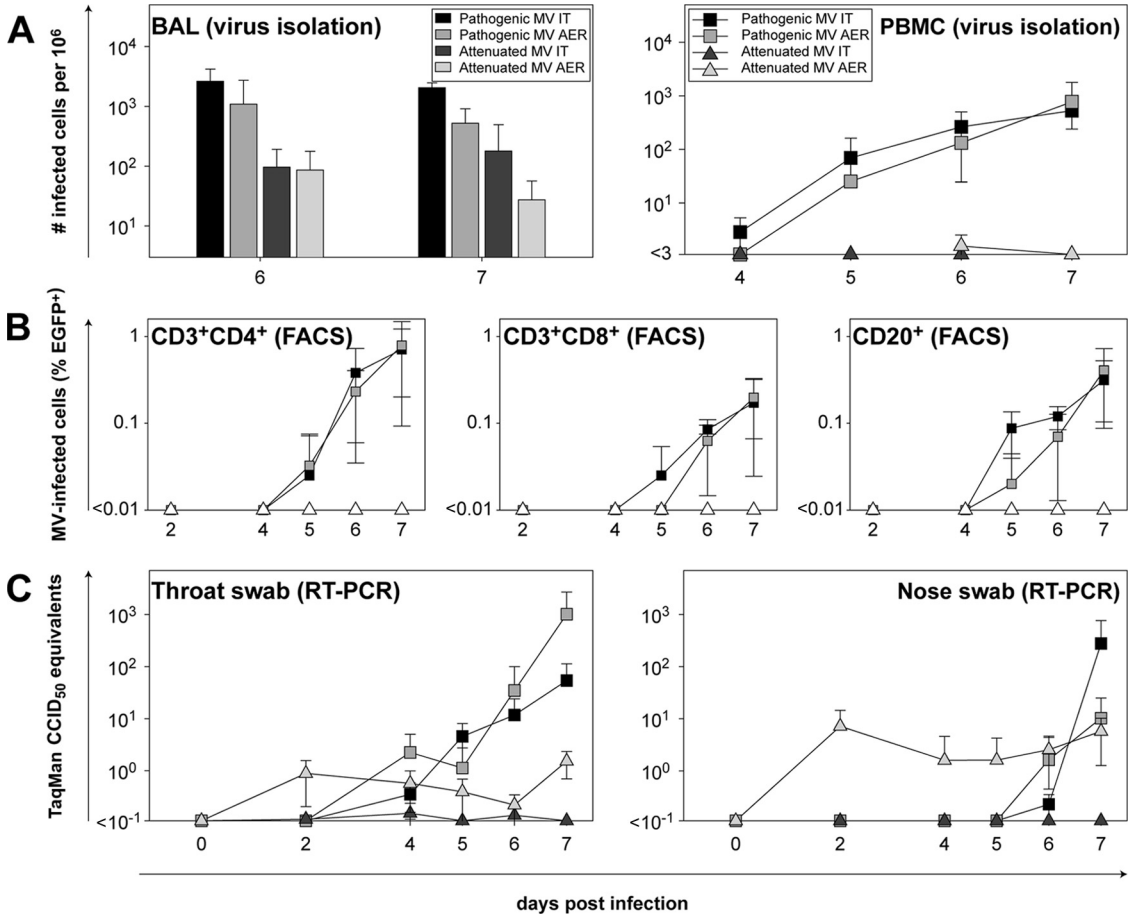

FIG. 2. Detection of MV in blood, lungs, throat, and nose. In all plots, the results are shown as means ± SD of the 4 animals within a group. (A) Virus isolations from BAL cells and PBMC. Virus was isolated in human B-LCL in an infectious-center assay, and the results are expressed as the number of infected cells per 10^6 total cells. AER, aerosol. (B) Flow cytometry of PBMC subpopulations. The data shown are the percentages $EGFP^+$ cells in the $CD3^+$ $CD4^+$, $CD3^+$ $CD8^+$, and $CD20^+$ subpopulations. FACS, fluorescence-activated cell sorter. (C) RT-PCR on throat and nose swabs. MV was detected by real-time RT-PCR on total RNA isolated from throat and nose swabs collected in transport medium.

aerosol-infected macaques to identify which cell types were infected by attenuated MV. The vast majority of cells infected with attenuated MV were $CD11c^+$, and several $CD11c^+$ multinucleated giant cells were observed (Fig. 5). While MV infection of the epithelium surrounding the alveoli was detected, cytokeratin immunostaining (AE1/AE3) was disrupted within foci of infected cells (Fig. 5). Furthermore, viral spread appeared to be predominantly mediated by cell-to-cell spread between intimately connected $CD11c^+$ cells. While $CD3^+$ T lymphocytes were abundantly present in the lungs, MV-infected T lymphocytes were rare and difficult to detect (Fig. 5). Finally, only low numbers of $CD20^+$ B lymphocytes were detected in the lung parenchyma (although lymphoid infiltrations in the lung did contain B lymphocytes), and MV-infected B lymphocytes could not be observed (Fig. 5).

Pathogenic MV infected similar cell types in general, although cytokeratin-positive infected epithelial cells were less frequently observed. Notably, more than 90% of EGFP-positive cells double stained with CD11c (Fig. 6). An important difference with the lungs of animals infected with attenuated MV was that large numbers of MV-infected T and B lymphocytes were observed, mostly within large areas of lymphoid tissue but rarely around the alveoli (Fig. 6).

DISCUSSION

In this study, we performed a side-by-side comparison of the *in vivo* tropism of attenuated and pathogenic MV in nonhuman primates after i.t. or aerosol delivery. In the lungs, both viruses predominantly infected $CD11c^+$ myeloid cells, which include alveolar macrophages and DC. Although we have tried different surface molecules as specific markers, we have been unsuccessful in discriminating DC or macrophages in formalin-fixed tissues. Only the pathogenic MV also caused viremia and was disseminated to lymphoid tissues, the respiratory submucosa, and the skin.

The aerosol route of infection more closely mimics a natural MV infection than i.t. delivery. For the pathogenic MV strain ($rMV^{IC323}EGFP$), no differences were observed in the virus isolation profiles from BAL cells, blood, throat, or nose samples between the two routes of infection. In addition, no macroscopic or microscopic differences in distribution or intensity

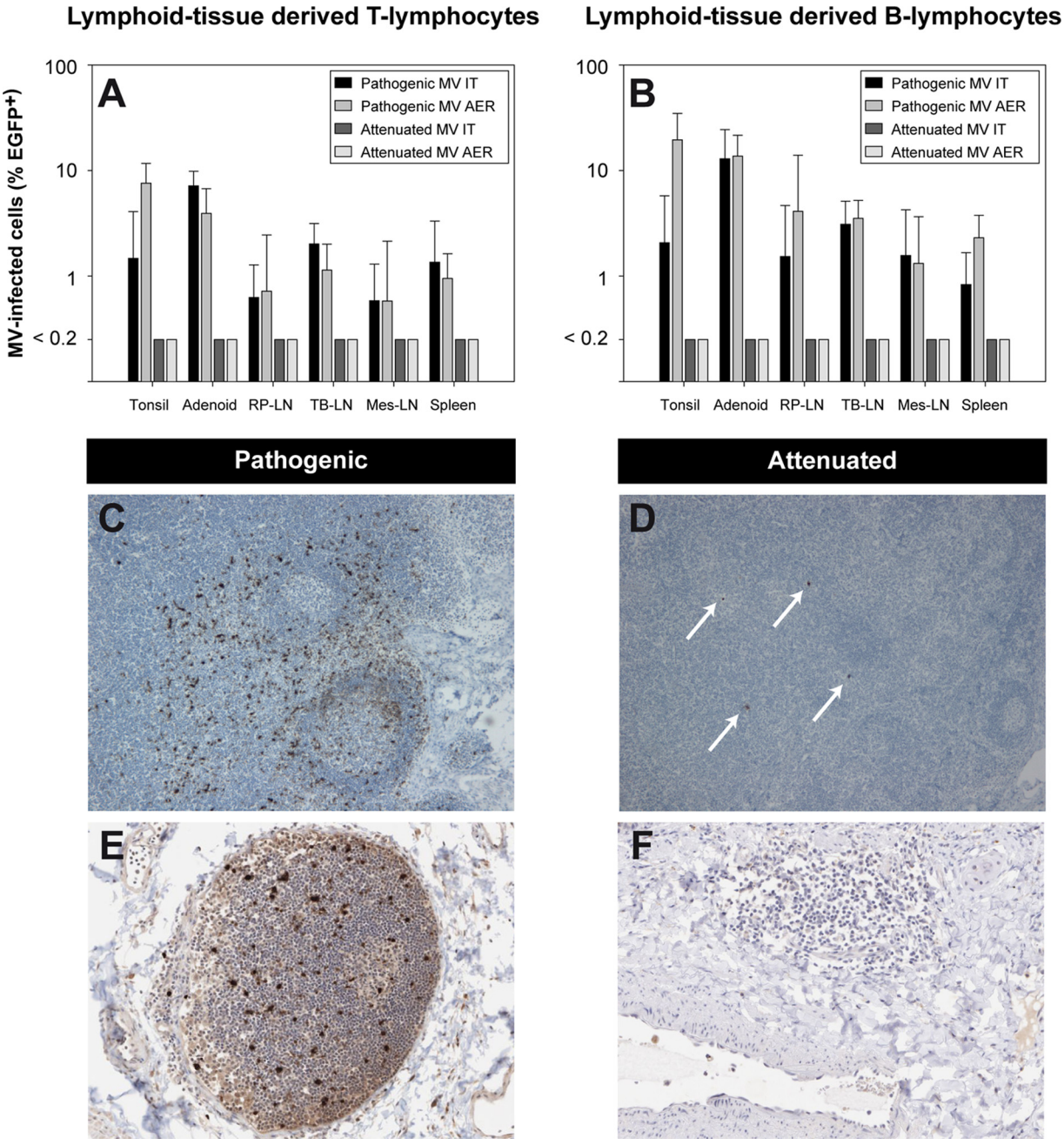

FIG. 3. Lymphoid infection by attenuated or pathogenic MV. (A and B) Percentages of EGFP$^+$ cells in lymphoid organs. The percentages of MV-infected cells were determined in single-cell suspensions from lymphoid organs by flow cytometry and are shown as geometric means ± SD from the 4 animals within a group. AER, aerosol; RP-LN, retropharyngeal lymph node; TB-LN, tracheobronchial lymph node; Mes-LN, mesenteric lymph node. (C and D) Detection of EGFP$^+$ cells in lymph nodes. Immunohistochemistry confirmed abundant MV-infected cells in lymphoid organs of pathogenic-MV-infected animals. Attenuated MV could be detected in only a few isolated cells from lymph nodes of two out of eight animals (see arrows in panel D). (E and F) Presence of lymphoid infiltrations in the lungs. In macaques infected with pathogenic MV, lymphoid infiltrations containing MV-infected cells were frequently observed in lung sections. In attenuated-MV-infected macaques, lymphoid infiltrations were less frequent and did not contain virus-positive cells.

of fluorescent cells were observed in affected organs during necropsies 7 days p.i. Further analysis of the samples taken from macaques infected via either delivery route identified the same major target cells described previously (9), with CD3$^+$ CD4$^+$ T lymphocytes predominantly infected in blood and CD20$^+$ B lymphocytes predominantly infected in lymphoid organs. In all tissues, multifocal infection was detected, characterized by the presence of interconnected EGFP$^+$ cells, strongly suggesting that the virus spread in a cell-to-cell manner, as observed for several other viruses (33).

We used rMV^{rEdt}EGFP as an attenuated strain of MV. This virus is a recombinant EGFP-expressing virus based on the

TABLE 1. Detection of MV antigen in different tissues by immunohistochemistry

Tissue[a]	Infection score[b]											
	Pathogenic MV (rMV^{IC3232}EGFP)						Attenuated MV (rMV^{rEdt}EGFP)					
	i.t.			Aerosol			i.t.			Aerosol		
	EP	SUB	IM	EP	SUB	IM	EP	SUB	IM	EP	SUB	IM
URT												
Nasal septum	−/−	−/−		−/−	−/+		−/−	−/+		−/−	−/−	
Nasal concha	−/−	−/+		−/+	+/+		−/−	−/+		−/−	+/+	
Trachea	+/+	+/++		−/+	−/++		ND/−	ND/−		−/−	−/−	
LRT												
1^0 Bronchus	−/−		−/−	−/+		+/+++	−/−		−/−	−/−		−/−
Upper lungs	−/−		−/+	−/−		+/+++	−/−		+/+	−/−		+/+
Int. lungs	−/−		−/−	−/−		+/++	−/−		−/+	−/−		+/+
Lower lungs	−/−		−/−	−/+		−/+	−/−		−/+	−/−		+/+
Lymphoid												
Tonsils			++/++			++/++			−/−			−/+
Adenoids			−/+			++/+++			ND/ND			ND/ND
RP − LN			ND/+++			++/+++			ND/−			−/+
TB − LN			+/+++			+/+++			−/−			−/+
Digestive tract												
Tongue	−/+	−/+		−/+	−/+++		−/−	−/−		−/−	−/−	
Stomach	−/−	++/++		−/−	++/++		−/−	−/−		−/−	−/−	

[a] URT, upper respiratory tract; LRT, lower respiratory tract; 1^0 bronchus, primary bronchus; Int., intermediate; RP-LN, retropharyngeal lymph node; TB-LN, tracheobronchial lymph node.

[b] MV infection in different cell types is indicated. EP, epithelium; SUB, submucosa; IM, immune cells. Scores for 2 animals per group are shown. −, absence of virus from all cell layers; +, sparse virus-infected cells; ++, moderate number of virus-infected cells with multinucleated giant cells (MNGC); +++, high numbers of virus-infected cells with MNGC; ND, not determined.

Edtag strain of MV. An important consideration in the use of Edtag for *in vivo* infections is previous studies that show that Edtag probably does not encode a functional V protein, due to many C-to-T transitions (10). Therefore, we corrected the P gene sequence by site-directed mutagenesis and rescued a recombinant virus with normal V protein expression. To determine whether the attenuated rMV^{rEdt}EGFP behaved like other laboratory-adapted MV strains, *in vitro* infection experiments were performed with Vero and stably transfected Vero-CD150 cells. As expected, Vero cells were efficiently infected by attenuated MV, but not by pathogenic MV, whereas Vero-CD150 cells were infected by both strains. This confirmed that the attenuated strain can use both CD46 and CD150 *in vitro*, whereas the pathogenic MV strain uses only CD150. Attenuated and pathogenic MV displayed similar tropism in primary human cells. Activated primary B and T lymphocytes and mature DC were efficiently infected, whereas only low levels of infection were observed in immature DC and macrophages. It is noteworthy that these cells all expressed CD46 at a high level but were infected inefficiently with the attenuated strain of MV. Strikingly, in these *in vitro* infections, attenuated MV reached higher infection percentages than pathogenic MV.

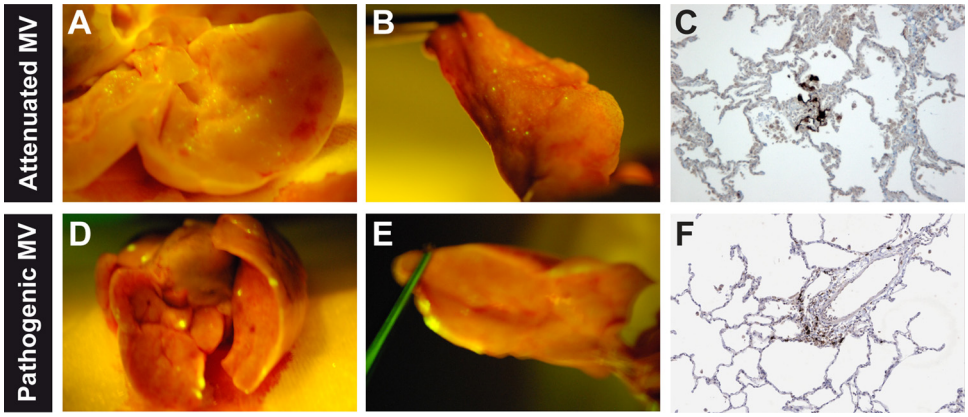

FIG. 4. Lung infection with attenuated or pathogenic MV. (A, B, D, and E) Macroscopic detection of EGFP fluorescence. (C and F) Microscopic detection of MV-infected cells with anti-EGFP (counterstained with hematoxylin).

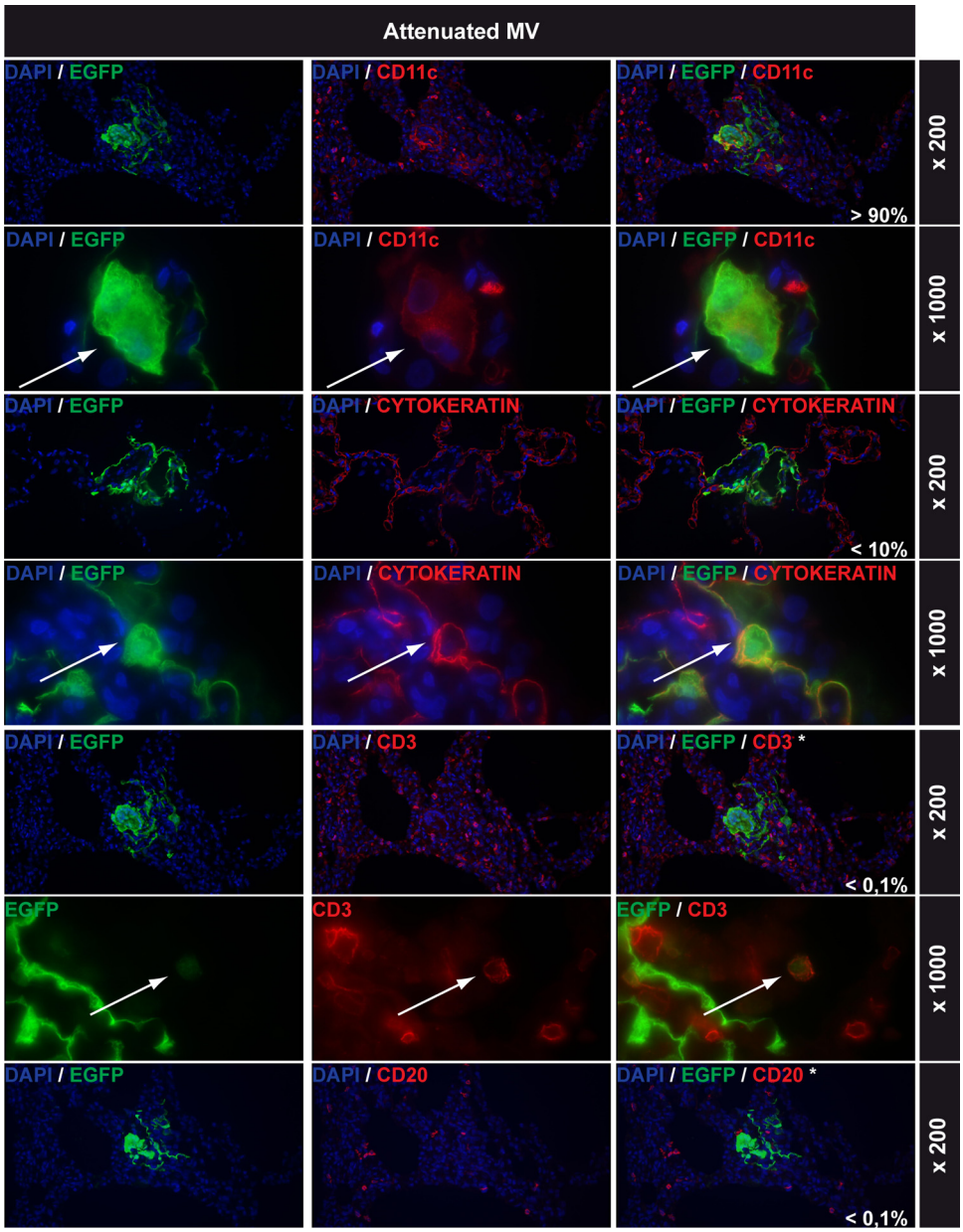

FIG. 5. Lung infections with attenuated MV: immunohistochemical double stainings. All rows show EGFP staining in green on the left, cell-type-specific staining in red in the middle (CD11c, cytokeratin, CD3, and CD20 for myeloid cells, epithelial cells, T lymphocytes, and B lymphocytes, respectively), and double staining on the right. DAPI counterstaining was used to identify nuclei. Magnifications are indicated on the right of each row. The percentages shown in white in the right-hand panels represent estimations of the relative contributions of these cell types to the total number of MV-infected cells in the lungs. Arrows indicate double-positive cells. Note that $EGFP^+$ cells shown in the CD3 and CD20 double stains are MV-infected $CD11c^+$ cells and that none of the $CD3^+$ or $CD20^+$ cells were $EGFP^+$.

This was not the case in primary macaque splenocytes, where pathogenic, but not attenuated, MV was able to spread and reached higher percentages at 4 days p.i. Overall, the percentages of infection were lower in the mixed splenocyte population than in the B and T lymphocytes and mature DC, probably due to the activation status of these cells. Previously, *ex vivo* infection of human tonsillar tissue with both recombinant pathogenic and attenuated MV strains also revealed that pathogenic MV infected most cell populations more efficiently (5).

It is important to note that rMV^{rEdt}EGFP is not completely identical to a live-attenuated MV vaccine strain. A sequence comparison was carried out between rMV^{rEdt}EGFP and the vaccine strains Moraten, Schwarz, Zagreb, Rubeovax, and AIK-C (GenBank accession numbers AF266287, AF266291, AF266290, AF266289, and AF266286, respectively). Analysis indicated that there were six amino acid changes in rMV^{rEdt}-EGFP that were not present in at least one of the vaccine strains: M (R175G), F (M94V), H (E492G), and L (E429D, R1629Q, and N1805S). The mutations in M, F, and H have

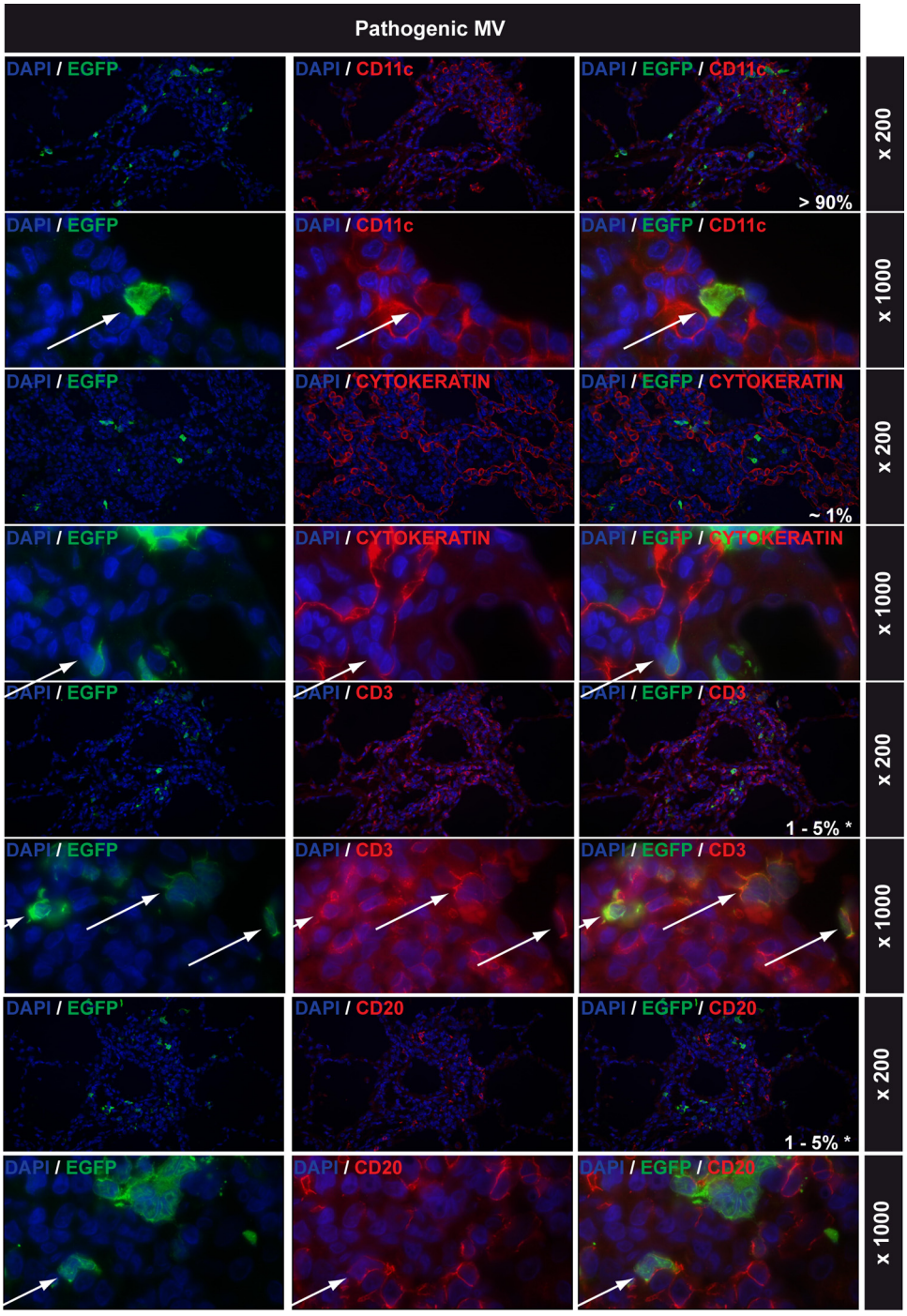

FIG. 6. Lung infections with pathogenic MV: immunohistochemical double stainings. For details, see the legend to Fig. 5. Note that infected lymphocytes were mainly found in lymphoid infiltrations in the lungs.

been investigated previously (31, 36, 38), on the basis of which it was decided not to change them to vaccine-identical amino acids. The changes in L either were outside the conserved domains (R1629Q) or the same changes were also retained in a previous study (E429D and N1805S) (10). It was therefore decided that it was not necessary to change them to vaccine-identical amino acids either. However, the possibility that part of our results may reflect specific properties of the Edtag strain cannot be excluded.

In macaques, pathogenic MV was detected in PBMC from all animals from 4 days p.i., whereas attenuated MV was detected only in PBMC from a single animal at 6 days p.i. These data are in good agreement with previous studies of macaques using nonrecombinant MV strains (3, 45). The most remark-

able parallel between attenuated and pathogenic MV was observed in the lungs. Attenuated MV was readily isolated from BAL cells 6 and 7 days p.i., albeit at lower levels than pathogenic MV. Immunohistochemical staining of infected lung tissue showed similar levels of infection, and dual staining indicated that the target cells in the lungs for both viruses were also similar. Attenuated and pathogenic MV predominantly infected $CD11c^+$ cells in the lungs, while MV-infected cytokeratin-positive epithelial cells were detected only occasionally. Lymphoid infiltrations in pathogenic-MV-infected macaques contained high levels of infected T and B lymphocytes. Whether these are sites of primary virus replication or are a consequence of viremia remains to be determined. The extent of infected epithelial cells in lung tissue has been previously described by Ludlow et al., with infection of the epithelium occurring only when MV was present in the underlying submucosa (24). Our data indicate that MV-infected cells of a nonepithelial origin are often present in the BAL or located in the lumen of alveoli, indicating that infection of epithelial cells may not be required for transmission of MV, as has been previously suggested (23).

One difference governed by the route of infection was observed in animals infected with attenuated MV. In the upper respiratory tract, pathogenic MV was detected only after infiltration of MV-infected $CD150^+$ cells following the onset of systemic viremia in both i.t. and aerosol infections. This is probably because infection of the airway epithelium from the apical side is not possible, and only low numbers of $CD150^+$ target cells are available. Infection of cytokeratin-positive epithelial cells was observed, however, possibly via the recently described putative epithelial cell receptor present on the basolateral sides of these cells (23, 37). Early detection of attenuated MV in the throat and nose after aerosol inhalation indicates that, in contrast to pathogenic MV, attenuated MV may be capable of primary replication in the upper respiratory tract. Such early replication might be mediated by the use of CD46 as an entry receptor. However, the presence of MV-infected cells could not be confirmed by immunohistochemistry, suggesting that the numbers of infected cells in the upper respiratory tract were low.

Our study was not designed as a vaccination study but as a comparative study of two MV strains with important biological differences. For this reason, we did not include the standard route of administration of live-attenuated MV vaccines in our experimental design. We are currently preparing for a vaccination study in which $rMV^{Edmonston\text{-}Zagreb}$ expressing EGFP will be administered to macaques via four routes of inoculation: subcutaneous injection, intratracheal inoculation, small-particle aerosol (for deep lung delivery), and large-particle aerosol (for upper respiratory tract delivery). In this study, animals will either be euthanized at early time points to assess virus tropism or be kept alive for monitoring of immune responses and assessment of protection from challenge infection.

In conclusion, we have shown that attenuated MV is capable of efficient replication in lymphoid cells *in vitro*, while replication in these cells is impaired *ex vivo* and *in vivo*. In addition, we show that even though attenuated MV is incapable of causing systemic infection, it causes a robust infection in the lungs of macaques. Most importantly, the cell types that are mainly targeted in the lungs are very similar to those targeted by pathogenic MV, and attenuated MV seems to prefer CD150 as a cellular entry receptor. It will be interesting to determine if this is the case in humans. There have been reports of progressive infection in vaccine recipients who have underlying immunological disorders (2, 25). Such tissues should be examined, as this would answer this question for the natural host and would also add to the weight of the macaque model as an ideal experimental-infection model for MV.

ACKNOWLEDGMENTS

We thank Beverley Craig, Robert Dias D'Ullois, Joan van der Lubbe, Werner Ouwendijk, Marleen Reedijk, Monique van Velzen, Joyce Verburgh, Leon de Waal, and Lot de Witte for practical assistance. We are grateful to Yusuke Yanagi for providing the Vero-CD150 cell line and the plasmid from which the $rMV^{IC323}EGFP$ virus was rescued. We thank Cees van Kooten for providing the CD40L-expressing cell line.

This work was supported by MRC (grant number G0801001), ZonMw (grant number 91208012), and the VIRGO Consortium, an innovative cluster approved by the Netherlands Genomics Initiative and partially funded by the Dutch government (grant number BSIK03012).

REFERENCES

1. **Allard, S. D., K. Pletinckx, K. Breckpot, C. Heirman, A. Bonehill, A. Michiels, C. A. Van Baalen, R. A. Gruters, A. D. M. E. Osterhaus, P. Lacor, K. Thielemans, and J. L. Aerts.** 2008. Functional T-cell responses generated by dendritic cells expressing the early HIV-1 proteins Tat, Rev, and Nef. Vaccine **26:**3735–3741.
2. **Angel, J. B., P. Walpita, R. A. Lerch, M. S. Sidhu, M. Masurekar, R. A. DeLellis, J. T. Noble, D. R. Snydman, and S. A. Udem.** 1998. Vaccine-associated measles pneumonitis in an adult with AIDS. Ann. Intern. Med. **129:**104–106.
3. **Auwaerter, P. G., P. A. Rota, W. R. Elkins, R. J. Adams, T. DeLozier, Y. Shi, W. J. Bellini, B. R. Murphy, and D. E. Griffin.** 1999. Measles virus infection in rhesus macaques: altered immune responses and comparison of the virulence of six different virus strains. J. Infect. Dis. **180:**950–958.
4. **Buckland, R., and T. F. Wild.** 1997. Is CD46 the cellular receptor for measles virus? Virus Res. **48:**1–9.
5. **Condack, C., J.-C. Grivel, P. Devaux, L. Margolis, and R. Cattaneo.** 2007. Measles virus vaccine attenuation: suboptimal infection of lymphatic tissue and tropism alteration. J. Infect. Dis. **196:**541–549.
6. **De Quadros, C. A., H. Izurieta, P. Carrasco, M. Brana, and G. Tambini.** 2003. Progress toward measles eradication in the region of the Americas. J. Infect. Dis. **187**(Suppl. 1)**:**S102–S110.
7. **De Swart, R. L.** 2009. Measles studies in the macaque model. Curr. Top. Microbiol. Immunol. **330:**55–72.
8. **De Swart, R. L., T. Kuiken, J. Fernandez de Castro, M. J. Papania, J. L. Valdespino, P. Minor, C. Witham, S. Yüksel, H. W. Vos, G. Van Amerongen, and A. D. M. E. Osterhaus.** 2006. Aerosol measles vaccination in macaques: preclinical studies of immune responses and safety. Vaccine **24:**6424–6436.
9. **De Swart, R. L., M. Ludlow, L. De Witte, Y. Yanagi, G. Van Amerongen, S. McQuaid, S. Yüksel, T. B. H. Geijtenbeek, W. P. Duprex, and A. D. M. E. Osterhaus.** 2007. Predominant infection of CD150+ lymphocytes and dendritic cells during measles virus infection of macaques. PLoS. Pathog. **3:**e178.
10. **Devaux, P., V. von Messling, W. Songsungthong, C. Springfeld, and R. Cattaneo.** 2007. Tyrosine 110 in the measles virus phosphoprotein is required to block STAT1 phosphorylation. Virology **360:**72–83.
11. **Dörig, R. E., A. Marcil, A. Chopra, and C. D. Richardson.** 1993. The human CD46 molecule is a receptor for measles virus (Edmonston strain). Cell **75:**295–305.
12. **Dubus, J. C., L. Vecellio, M. De Monte, J. B. Fink, D. Grimbert, J. Montharu, C. Valat, N. Behan, and P. Diot.** 2005. Aerosol deposition in neonatal ventilation. Pediatr. Res. **58:**10–14.
13. **El Mubarak, H. S., R. L. De Swart, A. D. M. E. Osterhaus, and M. Schutten.** 2005. Development of a semi-quantitative real-time RT-PCR for the detection of measles virus. J. Clin. Virol. **32:**313–317.
14. **El Mubarak, H. S., S. Yüksel, G. Van Amerongen, P. G. H. Mulder, M. M. Mukhtar, A. D. M. E. Osterhaus, and R. L. De Swart.** 2007. Infection of cynomolgus macaques (Macaca fascicularis) and rhesus macaques (Macaca mulatta) with different wild-type measles viruses. J. Gen. Virol. **88:**2028–2034.
15. **Enders, J. F., S. L. Katz, M. V. Milovanovic, and A. Holloway.** 1960. Studies on an attenuated measles-virus vaccine. I. Development and preparation of the vaccine: techniques for assay of effects of vaccination. N. Engl. J. Med. **263:**153–159.

16. **Enders, J. F., and T. C. Peebles.** 1954. Propagation in tissue cultures of cytopathic agents from patients with measles. Proc. Soc. Exp. Biol. Med. **86:**277–286.
17. **Fontana, J. M., B. Bankamp, W. J. Bellini, and P. A. Rota.** 2008. Regulation of interferon signaling by the C and V proteins from attenuated and wild-type strains of measles virus. Virology **374:**71–81.
18. **Garonne, P., E.-M. Neidhardt, E. Garcia, L. Galibert, C. van Kooten, and J. Banchereau.** 1995. Fas ligation induces apoptosis of CD40-activated human B lymphocytes. J. Exp. Med. **182:**1265–1273.
19. **Gould, E.** 1974. Variants of measles virus. Med. Microbiol. Immunol. **160:** 211–219.
20. **Griffin, D. E.** 2007. Measles virus, p. 1551–1585. *In* D. M. Knipe and P. M. Howley (ed.), Fields virology. Lippincott Williams & Wilkins, Philadelphia, PA.
21. **Hashimoto, K., N. Ono, H. Tatsuo, H. Minagawa, M. Takeda, K. Takeuchi, and Y. Yanagi.** 2002. SLAM (CD150)-independent measles virus entry as revealed by recombinant virus expressing green fluorescent protein. J. Virol. **76:**6743–6749.
22. **Hilleman, M. R.** 2001. Current overview of the pathogenesis and prophylaxis of measles with focus on practical implications. Vaccine **20:**651–665.
23. **Leonard, V. H. J., P. L. Sinn, G. Hodge, T. Miest, P. Devaux, N. Oezguen, W. Braun, P. B. McCray, M. B. McChesney, and R. Cattaneo.** 2008. Measles virus blind to its epithelial cell receptor remains virulent in rhesus monkeys but cannot cross the airway epithelium and is not shed. J. Clin. Invest. **118:**2448–2458.
24. **Ludlow, M., L. Rennick, S. Sarlang, G. Skibinski, S. McQuaid, T. Moore, R. L. De Swart, and W. P. Duprex.** 2010. Wild-type measles virus infection of primary epithelial cells occurs via the basolateral surface without syncytium formation or release of infectious virus. J. Gen. Virol. doi:10.1099/vir.0.016428-0.
25. **Moss, W. J., C. J. Clements, and N. A. Halsey.** 2003. Immunization of children at risk of infection with human immunodeficiency virus. Bull. World Health Organ. **81:**61–70.
26. **Naniche, D., G. Varior-Krishnan, F. Cervoni, T. F. Wild, B. Rossi, C. Rabourdin-Combe, and D. Gerlier.** 1993. Human membrane cofactor protein (CD46) acts as a cellular receptor for measles virus. J. Virol. **67:**6025–6032.
27. **Naniche, D., A. Yeh, D. S. Eto, M. Manchester, R. M. Friedman, and M. B. A. Oldstone.** 2000. Evasion of host defenses by measles virus: wild-type measles virus infection interferes with induction of alpha/beta interferon production. J. Virol. **74:**7478–7484.
28. **Ohno, S., N. Ono, M. Takeda, K. Takeuchi, and Y. Yanagi.** 2004. Dissection of measles virus V protein in relation to its ability to block alpha/beta interferon signal transduction. J. Gen. Virol. **85:**2991–2999.
29. **Patterson, J. B., D. Thomas, H. Lewicki, M. A. Billeter, and M. B. A. Oldstone.** 2000. V and C proteins of measles virus function as virulence factors in vivo. Virology **267:**80–89.
30. **Peebles, T. C., K. McCarthy, J. F. Enders, and A. Holloway.** 1957. Behavior of monkeys after inoculation of virus derived from patients with measles and propagated in tissue culture together with observations on spontaneous infections of these animals by an agent exhibiting similar antigenic properties. J. Immunol. **78:**63–74.
31. **Plemper, R. K., and R. W. Compans.** 2003. Mutations in the putative HR-C region of the measles virus F2 glycoprotein modulate syncytium formation. J. Virol. **77:**4181–4190.
32. **Radecke, F., P. Spielhofer, H. Schneider, K. Kaelin, M. Huber, C. Dotsch, G. Christiansen, and M. A. Billeter.** 1995. Rescue of measles viruses from cloned DNA. EMBO J. **14:**5773–5784.
33. **Sattentau, Q.** 2008. Avoiding the void: cell-to-cell spread of human viruses. Nat. Rev. Microbiol. **6:**815–826.
34. **Schwarz, A. J.** 1962. Preliminary tests of a highly attenuated measles vaccine. Am. J. Dis. Child. **103:**386–389.
35. **Stittelaar, K. J., T. Kuiken, R. L. De Swart, G. Van Amerongen, H. W. Vos, H. G. M. Niesters, P. van Schalkwijk, T. van der Kwast, L. S. Wyatt, B. Moss, and A. D. M. E. Osterhaus.** 2001. Safety of modified vaccinia virus Ankara (MVA) in immune-suppressed macaques. Vaccine **19:**3700–3709.
36. **Tahara, M., M. Takeda, F. Seki, T. Hashiguchi, and Y. Yanagi.** 2007. Multiple amino acid substitutions in hemagglutinin are necessary for wild-type measles virus to acquire the ability to use receptor CD46 efficiently. J. Virol. **81:**2564–2572.
37. **Tahara, M., M. Takeda, Y. Shirogane, T. Hashiguchi, S. Ohno, and Y. Yanagi.** 2008. Measles virus infects both polarized epithelial and immune cells using distinctive receptor-binding sites on its hemagglutinin. J. Virol. **82:**4630–4637.
38. **Tahara, M., M. Takeda, and Y. Yanagi.** 2005. Contributions of matrix and large protein genes of the measles virus Edmonston strain to growth in cultured cells as revealed by recombinant viruses. J. Virol. **79:**15218–15225.
39. **Takeda, M., K. Takeuchi, N. Miyajima, F. Kobune, Y. Ami, N. Nagata, Y. Suzaki, Y. Nagai, and M. Tashiro.** 2000. Recovery of pathogenic measles virus from cloned cDNA. J. Virol. **74:**6643–6647.
40. **Tatsuo, H., N. Ono, K. Tanaka, and Y. Yanagi.** 2000. SLAM (CDw150) is a cellular receptor for measles virus. Nature **406:**893–897.
41. **Tober, C., M. Seufert, H. Schneider, M. A. Billeter, I. C. Johnston, S. Niewiesk, V. Ter Meulen, and S. Schneider-Schaulies.** 1998. Expression of measles virus V protein is associated with pathogenicity and control of viral RNA synthesis. J. Virol. **72:**8124–8132.
42. **Valdespino-Gomez, J. L., M. De Lourdes Garcia-Garcia, J. Fernandez de Castro, A. M. Henao-Restrepo, J. Bennett, and J. Sepulveda-Amor.** 2006. Measles aerosol vaccination. Curr. Top. Microbiol. Immunol. **304:**165–193.
43. **Valsamakis, A., H. Schneider, P. G. Auwaerter, H. Kaneshima, M. A. Billeter, and D. E. Griffin.** 1998. Recombinant measles viruses with mutations in the C, V, or F gene have altered growth phenotypes in vivo. J. Virol. **72:**7754–7761.
44. **Van Binnendijk, R. S., M. C. M. Poelen, G. Van Amerongen, P. De Vries, and A. D. M. E. Osterhaus.** 1997. Protective immunity in macaques vaccinated with live attenuated, recombinant, and subunit measles vaccines in the presence of passively acquired antibodies. J. Infect. Dis. **175:**524–532.
45. **Van Binnendijk, R. S., R. W. J. van der Heijden, G. Van Amerongen, F. G. C. M. UytdeHaag, and A. D. M. E. Osterhaus.** 1994. Viral replication and development of specific immunity in macaques after infection with different measles virus strains. J. Infect. Dis. **170:**443–448.
46. **WHO.** 2009. Global reductions in measles mortality 2000–2008 and the risk of measles resurgence. Wkly. Epidemiol. Rec. **84:**509–516.
47. **Yanagi, Y., M. Takeda, and S. Ohno.** 2006. Measles virus: cellular receptors, tropism and pathogenesis. J. Gen. Virol. **87:**2767–2779.